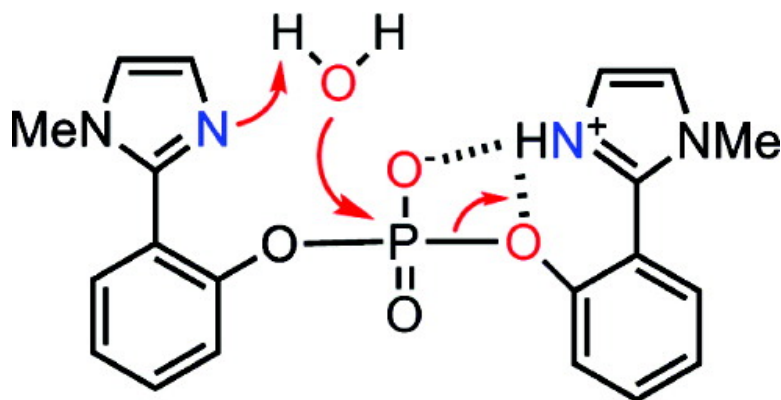


## Intramolecular Acid–Base Catalysis of a Phosphate Diester: Modeling the Ribonuclease Mechanism

Elisa S. Orth, Tiago A. S. Brando, Milagre, Marcos N. Eberlin, and Faruk Nome

*J. Am. Chem. Soc.*, **2008**, 130 (8), 2436-2437 • DOI: 10.1021/ja710693x

Downloaded from <http://pubs.acs.org> on February 8, 2009



### More About This Article

Additional resources and features associated with this article are available within the HTML version:

- Supporting Information
- Links to the 2 articles that cite this article, as of the time of this article download
- Access to high resolution figures
- Links to articles and content related to this article
- Copyright permission to reproduce figures and/or text from this article

[View the Full Text HTML](#)



## Intramolecular Acid–Base Catalysis of a Phosphate Diester: Modeling the Ribonuclease Mechanism

Elisa S. Orth,<sup>†</sup> Tiago A. S. Brandão,<sup>†</sup> Humberto M.S. Milagre,<sup>‡</sup> Marcos N. Eberlin,<sup>‡</sup> and Faruk Nome<sup>\*†</sup>

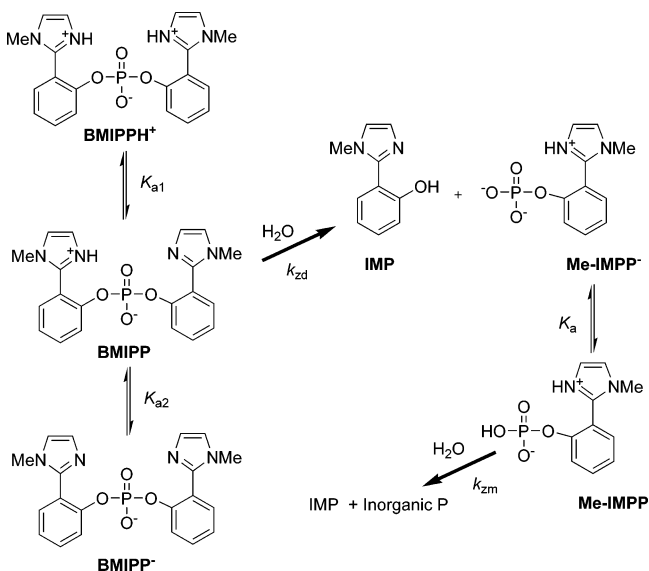
Universidade Federal de Santa Catarina, Florianópolis, SC 88040-900, Brazil. ThoMson Mass Spectrometry Laboratory, Institute of Chemistry, State University of Campinas, Campinas, SP, Brazil

Received November 29, 2007; E-mail: faruk@qmc.ufsc.br

The mechanism of ribonuclease A (RNase A) activity has been widely studied by evaluating different aspects such as roles of the catalytic amino acids, of different substrates, of thio effects, of organic solvents, and pH and temperature dependences.<sup>1</sup> The usually accepted mechanism is the general acid–base pathway where a deprotonated imidazole group acts as a general base and another protonated imidazole group acts as a general acid interacting with the leaving group. This “classical” mechanism has been questioned and a triester-like route has been considered with protonation of a nonbridging phosphoryl oxygen leading to a transition state resembling those typical of phosphate triester reactions.<sup>2</sup> Many bifunctional mimics have been studied, including oligonucleotides with imidazole residues<sup>3</sup> and cyclodextrins with imidazole groups attached to the sugar residues.<sup>4</sup> In the particular case of cyclodextrin mimics of RNase A, their catalytic efficiency is attributed not only to the imidazole groups but also to their hydrophobic binding to the substrate,<sup>5</sup> although the importance of the hydrophobic effects has been questioned, because catalytic effects are small for reactions of a variety of substrates with polymers with hydrophobic centers.<sup>6</sup> Although all these models resemble some aspects of RNase A reactions, they do not support fully the classical mechanism. We report the hydrolysis kinetics of a phosphate diester, (bis(2-(1-methyl-1*H*-imidazolyl)phenyl) phosphate) BMIPP, which bears two imidazole groups that may potentially act as the general acid–base catalysts conserved in the active site of RNase A (Scheme 1).

To probe the mechanism of BMIPP hydrolysis, we used our knowledge in similar<sup>7</sup> and related<sup>8</sup> studies and applied ESI-MS/(MS) in the negative ion mode to monitor the course of reaction. Reagents, intermediates, and products in anionic forms were transferred directly from the reaction solution to the gas phase, detected by ESI-MS, and then characterized by ESI-MS/MS via their unimolecular dissociation chemistry. After 25 min of hydrolysis of BMIPP in aqueous solution at pH 6.5 and 60 °C, a characteristic ESI-MS (Figure 1) was recorded. In this spectrum, a series of major anions are detected and identified as the anionic form of the reactant BMIPP of *m/z* 409, the monoester Me-IMPP of *m/z* 253, and the final phenolic product IMP of *m/z* 173, as well as inorganic P in the form of PO<sub>3</sub><sup>−</sup> of *m/z* 79 and H<sub>2</sub>PO<sub>4</sub><sup>−</sup> of *m/z* 97. Note the accurate mass measurements that corroborate the composition assignments. ESI-MS/MS was then used to characterize these important species via collision-induced dissociation. The resulting tandem mass spectra also supported the identifications: the Me-IMPP anion of *m/z* 253 is found to dissociate nearly exclusively to PO<sub>3</sub><sup>−</sup> of *m/z* 79 (Figure 2), deprotonated IMP of *m/z* 173 dissociates mainly by two routes that lead either to the fragment ion of *m/z* 158 by the loss of a methyl radical or the fragment of *m/z* 118 by likely the loss of 1-methyl-1*H*-azirine (C<sub>3</sub>H<sub>5</sub>N) thus forming the 2-cyanophenoxy anion (Figure 3). Therefore, ESI-MS and

Scheme 1



ESI-MS/MS data support the reaction pathway as depicted in Scheme 1.

Kinetics as a function of pH are shown in Figure 4, and reactions were followed spectrophotometrically at 290 nm with  $7.0 \times 10^{-5}$  M BMIPP. Figure 4 shows a bell-shaped pH-rate profile indicating bifunctional catalysis with a rate maximum at pH 6.5–6.8, where one imidazole group is protonated and another is deprotonated. The pH profile indicates that the monocationic (BMIPPH<sup>+</sup>) and monoanionic species (BMIPP<sup>−</sup>) are unreactive under our experimental conditions and hydrolysis of Me-IMPP<sup>−</sup> is sufficiently slow that it is the product at pH  $\geq 4$  (Scheme 1).

The data in Figure 4 were fitted with eq 1, derived from Scheme 1, giving  $k_{zd} = 1.98 \times 10^{-3}$  s<sup>−1</sup> for reaction of the zwitterionic species, with kinetic p*K*<sub>a</sub> values of 6.10 and 7.20 at 60 °C.

$$k_{\text{obs}} = k_{\text{zd}} \chi_{\text{BMIPP}} \quad (1)$$

Titration measurements at 25 °C confirmed this assumption, with p*K*<sub>a</sub> values of 6.2 and 7.8 for the acid dissociation of BMIPPH<sup>+</sup>–

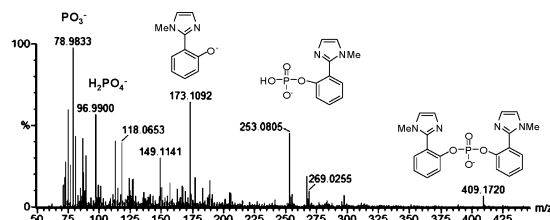


Figure 1. ESI-MS after 25 min of hydrolysis of BMIPP in aqueous solution at pH 6.5 and 60 °C.

<sup>†</sup> Universidade Federal de Santa Catarina.

<sup>‡</sup> State University of Campinas.

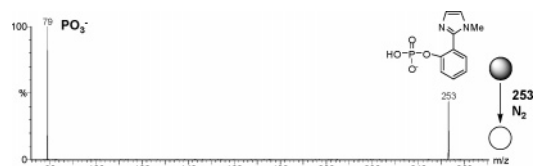


Figure 2. ESI-MS/MS of the Me-IMP anion of  $m/z$  253.

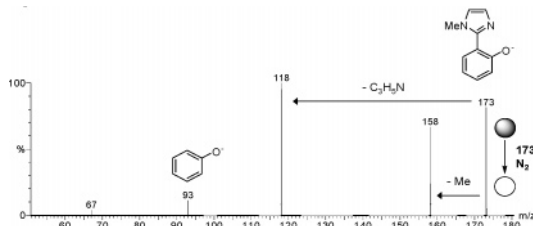


Figure 3. ESI-MS/MS of deprotonated IMP of  $m/z$  173.

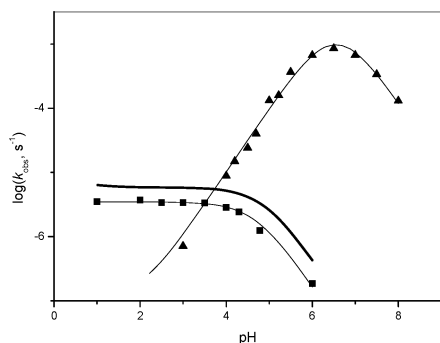
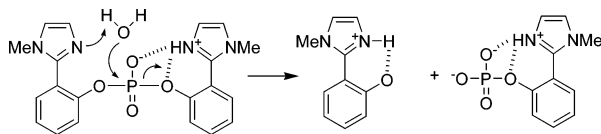


Figure 4. pH-rate profiles for the hydrolysis of BMIPP ( $\blacktriangle$ ) and Me-IMP ( $\blacksquare$ ), at 60 °C,  $\mu = 1.0$  (KCl). The solid lines for BMIPP and Me-IMP represent fits with eqs 1 and 2, respectively. The black solid line is the fit for hydrolysis of 2-(2'-imidazolium)phenyl phosphate (IMPP).<sup>9</sup>

#### Scheme 2. Mechanism Proposed for the Hydrolysis of BMIPP



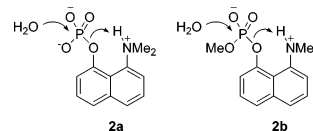
and BMIPP, respectively. The hydrolysis of BMIPPH<sup>+</sup> is slower than the hydrolysis of the zwitterionic form of Me-IMP, and the data for hydrolysis of the monoester in Figure 4 were fitted with eq 2, giving  $k_{zm} = 3.65 \times 10^{-6} \text{ s}^{-1}$  and  $\text{p}K_a = 4.52$ . The calculated rate and acid dissociation constant are similar to those reported for the hydrolysis of 2-(2'-imidazolium)phenyl phosphate (IMPP, solid line in Figure 4), indicating that the methyl group decreases slightly the catalytic efficiency of the imidazolium group.<sup>9</sup>

$$k_{\text{obs}} = k_{zm} \alpha_{\text{Me-IMP}} \quad (2)$$

The observed isotope kinetic effect,  $k_{\text{H}_2\text{O}}/k_{\text{D}_2\text{O}}$ , was 1.42, consistent with proton transfer in transition state formation and similar with values reported for other intramolecularly catalyzed phosphodiester hydrolysis reactions.<sup>9,10</sup> The activation parameters  $\Delta H^\ddagger = 19.0 \pm 1.2 \text{ kcal/mol}$  and  $\Delta S^\ddagger = -9.05 \pm 0.5 \text{ eu}$  calculated for the zwitterionic species of BMIPP, at pH 5.5–7.0 at each temperature, indicate a bimolecular hydrolysis mechanism, involving a water molecule in the transition state.<sup>9</sup>

The hydrolysis of BMIPP is considerably faster by a factor of  $10^6$ , than those of diphenyl phosphates with leaving groups of similar  $\text{p}K_a$  ( $\sim 7.85$ ),<sup>11a</sup> which is attributed to intramolecular general acid–base catalysis. It is important to notice that in the intramo-

lecular general acid catalysis by the dimethylammonium center in 8-dimethylamino-1-naphthyl phosphates **2a** and **2b**, the hydrolysis of the monoester **2a** is 18 times faster than that of the diester **2b**.<sup>10</sup>



Conversely, hydrolysis of the BMIPP diester is  $\sim 540$  times more reactive than the zwitterionic Me-IMP monoester. The result indicates important intramolecular general base catalysis as shown in Scheme 2. Similarly to the reaction of **2a**, we have no evidence to implicate a pentacovalent intermediate, and any such species would be very short-lived.<sup>10</sup>

The intramolecular catalytic efficiency of BMIPP is even more significant in comparisons with reactions involving cleavage of RNA and various derivatives by imidazole buffers that show enhancements of up to 3-fold,<sup>11b</sup> or the intramolecular hydrolysis of bis-(2-carboxyphenyl) phosphate, where was observed an unexpectedly low general acid catalysis, of only 4-fold.<sup>11c</sup>

In BMIPP, the distance between proton-accepting and -donating nitrogen atoms is ca. 7 Å (corresponding distances in RNase are  $\sim 6.5$  Å). Molecular models of the ground state of BMIPP show that the general acid is hydrogen bonded to both, the aryl oxygen and to one of the negatively charged nonbridging phosphoester oxygens. This initial state is consistent with reports of Anslyn et al.<sup>12</sup> for the guanidinium substituent as intramolecular general-acid catalyst in phosphoryl transfer reactions and observed a 40-fold rate enhancement relative to a reaction with proton transfer to the nonbridging phosphoester oxygen. The catalytic effect in BMIPP results from the combination of (i) favorable activation of a water molecule by general base catalysis and (ii) the concerted proton transfer from the general acid catalyst to the bridge oxygen atom, which requires simultaneous rotation of the imidazolium to approach planarity with the phenyl ring in the transition state. The detailed mechanism of the observed effect will be discussed in our full paper including density functional theory calculations.

**Acknowledgment.** We thank the Brazilian foundations CNPq, FAPESP, and FAPESP for financial assistance.

**Supporting Information Available:** Synthesis and characterization of bis(2-(1-methyl-1*H*-imidazolyl)phenyl)phosphate, BMIPP; tables of kinetic data. This material is available free of charge via the Internet at <http://pubs.acs.org>.

#### References

- (1) Raines, R. T. *Chem. Rev.* **1998**, *98*, 1045–1065.
- (2) Herschlag, D. *J. Am. Chem. Soc.* **1994**, *116*, 11631–11635.
- (3) Niittymäki, T.; Lonnerberg, H. *Org. Biomol. Chem.* **2006**, *4*, 15–25.
- (4) Breslow, R.; Doherty, J. B.; Guillot, G.; Lipsey, C. *J. Am. Chem. Soc.* **1978**, *100*, 3227–3229.
- (5) Breslow, R.; Anslyn, E. V. *J. Am. Chem. Soc.* **1989**, *111*, 5972–5973.
- (6) Liu, L.; Rozenman, M.; Breslow, R. *J. Am. Chem. Soc.* **2002**, *124*, 12660–12661.
- (7) (a) Domingos, J. B.; Longhinotti, E.; Brandão, T. A. S.; Santos, L. S.; Eberlin, M. N.; Bunton, C. A.; Nome, F. *J. Org. Chem.* **2004**, *69*, 7898–7905. (b) Domingos, J. B.; Longhinotti, E.; Brandão, T. A. S.; Santos, L. S.; Eberlin, M. N.; Bunton, C. A.; Nome, F. *J. Org. Chem.* **2004**, *69*, 6024–6033.
- (8) (a) Santos, L. S.; Pavam, C. H.; Almeida, W. P.; Coelho, F.; Eberlin, M. N. *Angew. Chem. Int. Ed.* **2004**, *43*, 4330–4333. (b) Santos, L. S.; Rosso, G. B.; Pilli, R. A.; Eberlin, M. N. *J. Org. Chem.* **2007**, *72*, 5809–5812.
- (9) Brandão, T. A. S.; Orth, E. S.; Rocha, W. R.; Bortoluzzi, A. J.; Bunton, C. A.; Nome, F. *J. Org. Chem.* **2007**, *72*, 3800–3807.
- (10) Kirby, A. J.; Lima, M. F.; Silva, D.; Roussex, C. D.; Nome, F. *J. Am. Chem. Soc.* **2006**, *128*, 16944–16952.
- (11) (a) Kirby, A. J.; Younas, M. *J. Chem. Soc. B* **1970**, 510–513. (b) Kirby, A. J.; Marriott, R. E. *J. Am. Chem. Soc.* **1995**, *117*, 833–834. (c) Kirby, A. J.; Abell, K. W. Y. *J. Chem. Soc., Perkin Trans. 2* **1983**, *8*, 1171–1174.
- (12) Anslyn, E. V.; Piatek, A. M.; Gray, M. *J. Am. Chem. Soc.* **2004**, *126*, 9878–9879.

JA710693X